

# Biogeochemical controls on mercury methylation in the Allequash Creek wetland

Joel E. Creswell<sup>1,3</sup> · Martin M. Shafer<sup>1,4</sup> · Christopher L. Babiarz<sup>1,2</sup> · Sue-Zanne Tan<sup>1</sup> · Abbey L. Musinsky<sup>1</sup> · Trevor H. Schott<sup>1</sup> · Eric E. Roden<sup>1,5</sup> · David E. Armstrong<sup>1</sup>

Received: 11 October 2016 / Accepted: 24 April 2017 / Published online: 13 May 2017  
© Springer-Verlag Berlin Heidelberg 2017

**Abstract** We measured mercury methylation potentials and a suite of related biogeochemical parameters in sediment cores and porewater from two geochemically distinct sites in the Allequash Creek wetland, northern Wisconsin, USA. We found a high degree of spatial variability in the methylation rate potentials but no significant differences between the two sites. We identified the primary geochemical factors controlling net methylmercury production at this site to be acid-volatile sulfide, dissolved organic carbon, total dissolved iron, and porewater iron(II). Season and demethylation rates also appear to regulate net methylmercury production. Our equilibrium speciation modeling demonstrated that sulfide likely regulated methylation rates by controlling the speciation of inorganic mercury and therefore its bioavailability to methylating bacteria. We found that no individual geochemical parameter could explain a significant amount of the observed

variability in mercury methylation rates, but we found significant multivariate relationships, supporting the widely held understanding that net methylmercury production is balance of several simultaneously occurring processes.

**Keywords** Mercury · Methylation · Bioavailability · Biogeochemistry · Hyporheic zone · Wetland · Speciation

## Introduction

Wetland environments are active regions of mercury methylation and can be the primary source of methylmercury to many aquatic systems (Hurley et al. 1995; St. Louis et al. 1996). Understanding the methylation process in these systems is vital for prediction and modeling of methylmercury (MeHg) accumulation within aquatic food webs. While mercury methylation is known to be carried out by sulfate-reducing bacteria, and to a lesser extent, iron-reducing bacteria in wetland systems (Compeau and Bartha 1985; Gilmour et al. 1992; Warner et al. 2003; Kerin et al. 2006), the geochemical controls on methylmercury production are not well understood (Benoit et al. 2003; Mitchell et al. 2008a, b; Schaefer and Morel 2009). In order for mercury methylation to occur in wetland environments, favorable conditions for sulfate- and iron-reducing bacteria need to be present, including a supply of labile organic carbon, an electron acceptor ( $\text{SO}_4^{2-}$  or  $\text{Fe(III)}$ ), and anoxia. In addition, a bioavailable source of inorganic  $\text{Hg(II)}$  is necessary. This bioavailability is hypothesized to be controlled primarily by speciation with sulfide (Benoit et al. 1999a, 2001; Deonarine and Hsu-Kim 2009; Zhang et al. 2012) and organic matter (Miskimmin et al. 1992; Driscoll et al. 1995; Barkay et al. 1997; Schaefer and Morel 2009). While it was long believed that sulfide could outcompete organic matter for mercury binding in sulfidic

Responsible editor: Philippe Garrigues

**Electronic supplementary material** The online version of this article (doi:10.1007/s11356-017-9094-2) contains supplementary material, which is available to authorized users.

✉ Joel E. Creswell  
joel.creswell@mail.house.gov

<sup>1</sup> Environmental Chemistry and Technology Program, University of Wisconsin – Madison, 660 N. Park St, Madison, WI 53706, USA

<sup>2</sup> Present address: Wisconsin Water Science Center, U.S. Geological Survey, 8505 Research Way, Middleton, WI 53562, USA

<sup>3</sup> U.S. House of Representatives, 2346 Rayburn House Office Building, Washington DC 20515, USA

<sup>4</sup> Wisconsin State Laboratory of Hygiene, 2601 Agriculture Dr, Madison, WI 53718, USA

<sup>5</sup> Department of Geoscience, University of Wisconsin – Madison, 1215 W. Dayton St, Madison, WI 53706, USA

environments, more recent research has shown a range of Hg-organic matter stability constants, some of which are much higher than those for Hg-sulfide interactions (Ravichandran 2004; Miller et al. 2007; Drott et al. 2007; Skyllberg 2008). In addition, organic matter can inhibit the aggregation of Hg-S complexes into clusters and nanoparticles, preventing precipitation and keeping Hg in a bioavailable state (Deonarine and Hsu-Kim 2009; Graham et al. 2012; Zhang et al. 2012). The result is most likely that both sulfide and strong organic ligands compete for mercury binding and that both control its bioavailability to methylating bacteria.

In this study, we collected sediment and porewater from two geochemically distinct sites, each with different redox conditions, within a northern Wisconsin wetland, and measured methylation rate potentials and a suite of related geochemical parameters. The goals of the work were to (1) quantify the spatial and seasonal variability of methylmercury production in this system; (2) examine a range of parameters related to mercury bioavailability and controls on methylation, including sulfide and dissolved organic matter; and (3) compare results to model simulations of mercury speciation to determine the dominant controls on bioavailability.

We chose the Allequash Creek wetland site because it is well studied and the dominant groundwater flow paths have

been identified, as is detailed below. By examining the factors contributing to methylmercury production in a well-characterized system, including iron, dissolved organic carbon, and sulfide, this study fills a knowledge gap relating to the impact of groundwater chemistry on the mercury cycle.

## Materials and methods

### Sampling sites

Allequash Creek is a groundwater-dominated stream in the Northern Highland Lake District of Wisconsin that has been well characterized by previous investigators (Krabbenhoft et al. 1995; Pint et al. 2003; Walker et al. 2003; Lowry et al. 2007; Kerr et al. 2008; Creswell et al. 2008). It falls within the study areas of two long-term efforts, the North Temperate Lakes Long-Term Ecological Research area and the U.S. Geological Survey's Water, Energy, and Biogeochemical Budgets.

We investigated two sites (Fig. 1). The upper springs site is a ~10-ha pond fed by groundwater discharges (Krabbenhoft et al. 1995; Pint et al. 2003) that makes up the headwaters of the stream. It is surrounded by woody wetland plants and

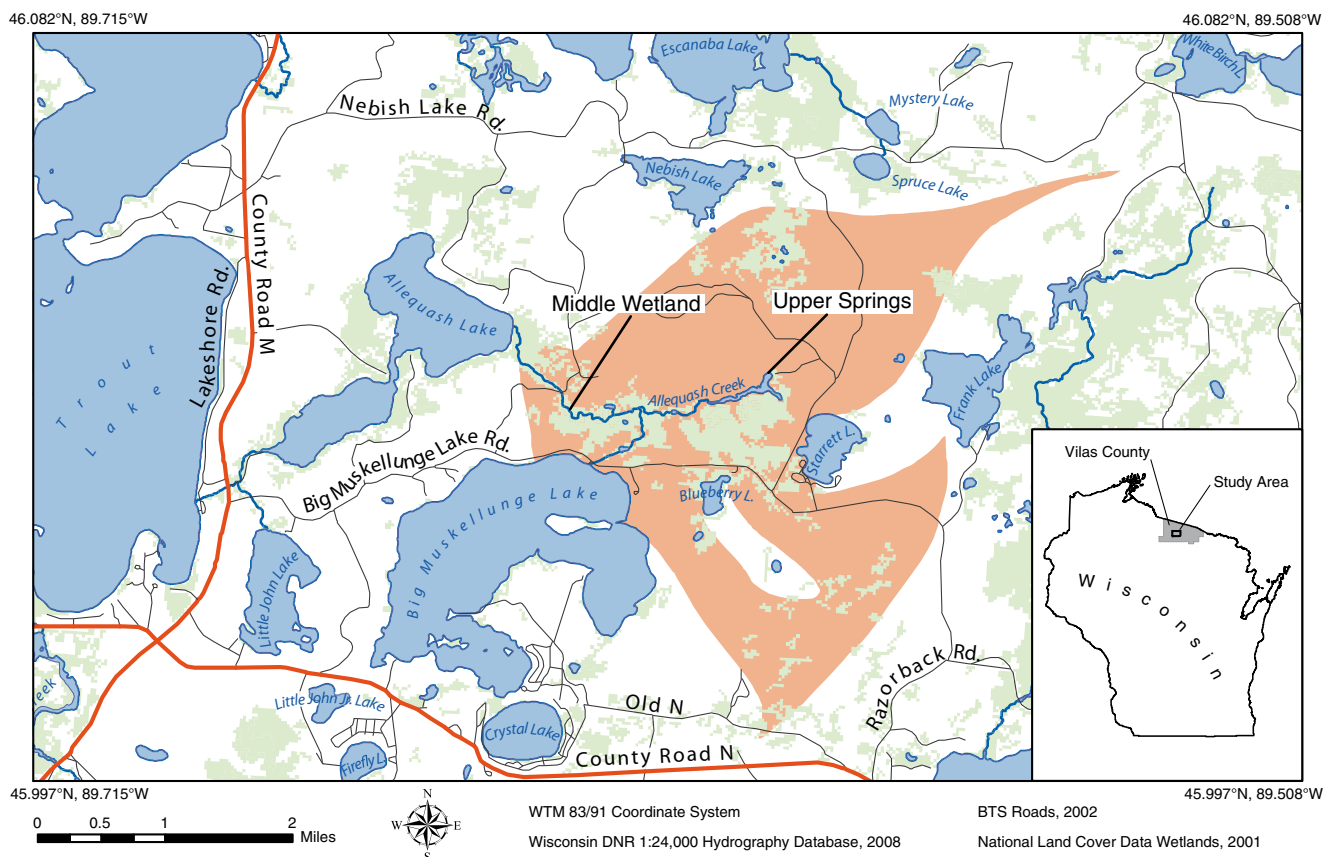


**Fig. 1** Map of sampling sites. Wetlands are shown in *light green*. The groundwater capture zone for Allequash Creek, based on Pint et al. (2003), is shown in *orange*

mixed spruce and deciduous forest. The soils in this area are mineral-dominated, and the groundwater discharging through them is relatively young and has a higher redox potential (i.e., is less-reducing). The middle wetland site is located in the peat-rich riparian section of the watershed, which is characterized by older groundwater discharge and a lower redox potential (i.e., more-reducing conditions). The stream here flows primarily through a single channel with a muddy bottom and has several smaller side channels and rivulets. The wetland adjacent to the channels is dominated by leatherleaf, sedge, and sphagnum moss (Krabbenhoft et al. 1995). These sites were selected for their distinct geochemical characteristics and groundwater ages (Table 1).

**Sampling**

To capture seasonal variability, we conducted field campaigns in July, 2008, October, 2008, February, 2009, and July, 2009. We were unavailable to collect samples in Spring, 2009. Four cores were collected from the hyporheic sediment of each site for sectioning and chemical analysis, and two from each site were collected and kept intact for measurement of mercury methylation and demethylation rates. Multiple cores were collected, all from within 1 m of one another, in order to average out spatial variability, not to capture any spatial patterns. We collected cores by hand in sharpened polycarbonate tubes. Each core included at least 10 cm of sediment and some overlying water to minimize redox changes in the upper sediment horizon. Cores were collected from areas of undisturbed sediment within the streambed, and efforts were made to maintain

an intact sediment-water interface. We followed strict trace metal clean techniques (Shafer et al. 1999).

Cores for chemical analysis were sectioned promptly within an anaerobic chamber. Each core was divided into five 2-cm sections which were composited by depth horizon in centrifuge bottles. Porewaters were separated from the sediments by centrifuging and were then passed through acid-cleaned 0.45-µm filters to remove remaining particulate material. Centrifuging was not carried out in an anoxic environment; however, the threads of the centrifuge bottles were wrapped with polytetrafluoroethylene (PTFE) tape and tightly sealed before being removed from the anaerobic chamber in order to minimize oxygen penetration. The entire core sectioning procedure was completed in less than 4 h, and cores awaiting processing were maintained at the ambient porewater temperature of the sampling site.

**Mercury methylation and demethylation rate potentials**

The incubation approach for this procedure was modeled after that of Hammerschmidt and Fitzgerald (2004), and the analysis followed the method of Hintelmann et al. (1995). All cores were kept intact throughout the incubation to minimize disturbance to the sediment microbial community. The cores for methylation rate potential measurements were injected with pH-neutral amendments of isotopically enriched <sup>200</sup>Hg(II), which were diluted to the appropriate concentration using Allequash Creek water. Cores for demethylation rate measurements were injected with isotopically enriched amendments of Me<sup>199</sup>Hg, prepared in the same way. Native water was used to

**Table 1** Porewater geochemistry of sampling sites

	Upper springs			Middle wetland		
	Range	Median	n =	Range	Median	n =
pH	7.3–8.7	8.2	17	7.5–8.7	8.1	20
Sulfate (µM)	0.01–59.2	13.8	20	0.0–12.1	2.92	20
Sulfide (µM)	<0.13–12.4	0.41	20	0.02–4.3	0.35	20
Total dissolved sulfur (µM)	4.4–61.5	38.7	20	2.39–32.5	4.28	20
% sulfide <sup>a</sup>	<0.13–59.4	1.62	20	0.1–66.6	8.59	20
Acid-volatile sulfide (µmol/kg)	0.0–580.3	41.0	20	0.0–563.6	54.7	18
Fe(II) (µM)	0.2–4.7	1.36	20	2.4–142.6	13.3	20
Total dissolved Fe (µM)	0.68–4.27	1.40	20	30.6–294	52.8	20
Total mercury (pM)	15.5–251	107	20	14.1–197	53.8	20
Total mercury (ng/L)	3.11–50.3	21.5	20	2.83–39.5	10.8	20
Methylmercury (pM)	<1.5–4.20	1.10	20	<1.5–8.91	2.46	20
Methylmercury (ng/L)	<0.30–0.842	0.221	20	<0.30–1.79	0.493	20
Dissolved organic carbon (mM)	0.19–0.50	0.26	20	0.13–1.77	0.26	19
Groundwater age <sup>b</sup> (year)	25–50			50–150		

<sup>a</sup> Percentage of total dissolved sulfur measured as sulfide

<sup>b</sup> (Pint et al. 2003)

allow the mercury amendments to achieve speciation comparable to what exists in situ; however, it is still assumed that the added mercury is more readily available to bacteria than native mercury within the core. Hence, these measurements are considered rate potentials, rather than actual rates.

Injections were made through silicone septa in the walls of the core tubes. The septa were spaced at 2-cm intervals starting 1 cm below the sediment-water interface. Each injection was distributed throughout the core horizon using the syringe needle to minimize channel effects. Amendments typically increased the total mercury (HgT) and MeHg burden of the sediment by 1–2%. All cores were incubated in the dark at the same temperature as the wetland porewater, measured at the time of sampling. Cores for methylation rate measurements were incubated for 8–22 h, and cores for demethylation rate measurements were incubated for 5–12 h. Incubations were terminated by slicing the core and freezing the subsections. Samples were stored frozen in acid-cleaned polypropylene vials until analysis.

Prior to analysis, small aliquots (0.5–1 g) of sediment were transferred to Teflon vessels and steam distilled following the method of Horvat et al. (1993), modified to include the addition of 1 mL 1 M CuSO<sub>4</sub> to each vessel prior to distillation. The aim of the CuSO<sub>4</sub> addition was to saturate strong MeHg-binding ligands in the sample matrix and improve MeHg recovery (Olson et al. 1997). Distilled samples were analyzed by aqueous ethylation, purge and trap, gas chromatographic separation, pyrolysis, and cold vapor atomic fluorescence detection, following EPA Method 1630 (U.S. Environmental Protection Agency 2001a). The cell outlet from the cold vapor atomic fluorescence spectrometer (Tekran 2500, Toronto, Canada) was connected to an inductively coupled-plasma mass spectrometer (ICP-MS; initially a PerkinElmer Elan 6100, later a PerkinElmer Elan DRC II, Waltham, MA) via a custom-machined Kynar fitting designed to mimic that of Hintelmann and Evans (1997). Signals from the ICP-MS were captured and integrated using THE PerkinElmer Chromera software, and peak areas were used for all subsequent calculations.

The ICP-MS was calibrated and its mass bias accounted for by the analysis of mercury standards of known concentration and isotopic composition (Blum and Bergquist 2007). The concentrations of methylmercury from the isotopically enriched amendments were calculated using measured ratios of enriched to unenriched isotopes in the samples, and the known isotopic abundance of natural and amended mercury. This method, when performed alongside a calibration, allows the simultaneous determination of natural and amended methylmercury concentrations, with corrections for isotopic impurities in the amendments (the Me<sup>199</sup>Hg amendment was 92% pure, and the <sup>200</sup>Hg amendment was 96% pure) (Hintelmann et al. 1995). Hg isotopes 196 and 204 were below the detection limit of the ICP-MS; their abundances in measured

samples were assumed to follow the natural isotopic distribution of mercury. Isotope 202 was used to determine the concentration of natural mercury in the sediment. Average detection limits and precision for relevant isotopes were as follows (det. limit / precision): <sup>199</sup>Hg—11.9 pg / 14.2%, <sup>200</sup>Hg—12.2 pg / 13.6%, and <sup>202</sup>Hg—12.7 pg / 12.8%.

### Porewater Hg and MeHg

Filtered porewater samples for total mercury and methylmercury analysis were preserved in the anaerobic chamber with 1% bromine monochloride (BrCl) and 1% trace metal grade hydrochloric acid, respectively, and were stored in Teflon containers. Analysis was carried out following established procedures (Babiarz et al. 1998; U.S. Environmental Protection Agency 2001a, 2002). The average detection limit for total mercury was 23.9 pg and the average analytical precision was 7.2%. For methylmercury, the average detection limit was 6.1 pg and the average analytical precision was 10.3%.

### Sediment total Hg

Sediment total mercury digestions were carried out on freeze-dried samples taken from each core horizon after porewater extraction. Aliquots of roughly 500 mg were precisely weighed into 100-mL volumetric flasks and were digested in 7 mL of a 5:2 (v/v) mixture of trace metal grade nitric acid and sulfuric acid. Flasks were heated to a slow boil until brown fumes ceased to evade from solution (approximately 6 h) (Bloom 1992; U.S. Environmental Protection Agency 2001b). Acid-cleaned glass marbles were used as pressure relief valves on the tops of the digestion flasks. The average detection limit was 1.1 ng/g and the analytical precision was 6.7%. Two certified reference materials were analyzed to confirm accuracy. The average recovery for the MESS-2 marine sediment material was 92.4% and that for the NIST-8406 Tennessee River sediment material was 83.9%.

### Sn-reducible Hg titrations

This method provided an estimate of the concentration of strong, mercury-binding organic ligands in porewater. Although the method is described in detail elsewhere (Lamborg et al. 2003), a brief description follows. Filtered porewater samples were evenly split into 6–8 subsamples, were amended with a range of Hg(II) concentrations between 0 and 10 µg/L, and were allowed to equilibrate overnight. Samples were reduced with stannous chloride (SnCl<sub>2</sub>) and purged with nitrogen, and the evaded Hg<sup>0</sup> was measured. By omitting any sample digestion before analysis, we assume this process allows the native Hg-organic speciation to remain intact and only allows those aqueous complexes of Hg that are kinetically labile, or have relatively weak equilibrium

coefficients ( $\log K \leq 19$ ), to be measured. The ligand concentrations are calculated from the difference between introduced and measured Hg by fitting a non-linear regression to the data. We fit a function of the form  $y = ax / (1 + bx)$  to a plot of the experimental data in the form of  $[\text{Hg}_{\text{added}}] - [\text{Hg}_{\text{measured}}]$  versus  $[\text{Hg}_{\text{measured}}]$ , using the “Modified Hyperbola I” algorithm in SigmaPlot 10 (Systat Software, Inc., San Jose, CA). The coefficients of the regression can be used to calculate an estimate of the total strong, mercury-binding organic ligand concentration,  $[\text{L}_T]$ , and the conditional stability constant of the Hg-L complex,  $K''$  (Gerringa et al. 1995; Hoffmann 2002). In order to convert the  $K'' = \frac{[\text{HgL}]}{[\text{Hg(II)}][\text{L}^{2-}]}$  values estimated by the titration to more conventional  $K' = \frac{[\text{HgL}]}{[\text{Hg}^{2+}][\text{L}^{2-}]}$  values, we estimated  $\alpha$ , the ratio of total Hg(II) to  $\text{Hg}^{2+}$  associated with inorganic complexes, using MINEQL+ (Schecher and McAvoy 2002).

In order to minimize the impact of sulfide on mercury speciation, and thus measure only the organic mercury-binding capacity of the porewater, samples were stored under oxic conditions, causing all sulfide in the porewater to be oxidized. Sulfide concentrations were confirmed to be below the detection limit in a subset of samples prior to analysis.

#### Additional geochemical measurements

Sulfate was measured electrochemically by ion chromatography, using a Dionex LC25/ED50/GP50 system with an average detection limit of 5.69  $\mu\text{M}$  and analytical precision of 5.21%. Dissolved Fe(II) (Stookey 1970) and sulfide (Cline 1969) concentrations were measured colorimetrically with average detection limits of 0.31 and 0.060  $\mu\text{M}$ , respectively, and average analytical precision of 4.04 and 10.4%, respectively. Sediment acid-soluble Fe(II) and Fe(III) were measured colorimetrically in a 0.5-N HCl solution (Lovley and Phillips 1986), with the difference between oxidized and reduced iron being determined by measurement before and after reduction of the sample with hydroxylamine hydrochloride (Viollier et al. 2000). The analytical performance was the same as for dissolved Fe(II). Dissolved organic carbon (DOC) was measured as non-purgeable organic carbon using a Shimadzu TOC-V/CSH organic carbon analyzer, with an average detection limit of 0.045 mM and average analytical precision of 3.61%. Total dissolved iron and sulfur were measured by high-resolution ICP-MS, using a Thermo Element 2 magnetic sector field instrument with an average detection limit of  $6.9 \times 10^{-3}$  and 0.19  $\mu\text{M}$ , respectively, and average analytical precision of 3.49 and 3.36%, respectively. pH was measured electrochemically using a handheld microelectrode. Acid-volatile sulfide (AVS) was measured in whole sediment by acidifying

samples in sealed vials, purging with nitrogen, and capturing evaded  $\text{H}_2\text{S}$  in 10% zinc acetate traps, following Fossing and Jørgensen (1989). The captured sulfide (as ZnS) was redissolved in reagent water and measured colorimetrically, as above. Percent loss on ignition (%LOI), a measure of the organic content of the sediment, was calculated as the mass difference between sediments dried overnight at 110 °C and combusted for at least 1 h at 450 °C.

#### Terminal electron accepting processes (TEAPs)

This method involves the use of a radiolabeled microbial substrate ( $2\text{-}^{14}\text{C}$ -acetate) to determine microbial productivity in the presence and absence of sodium molybdate ( $\text{NaMoO}_4$ ), a specific inhibitor of sulfate reduction. It is described in detail elsewhere (Lovley 1997; Warner et al. 2003), but a brief description follows. Two-milliliter aliquots of sediment from each core horizon were transferred to glass vials in the anaerobic chamber, which were flushed with  $\text{N}_2$  to remove hydrogen (a component of the chamber atmosphere) from the headspace and sealed.  $\text{H}_2$  removal avoids stimulating the microbial community with a substrate other than the labeled acetate. Vials were collected as paired duplicates, and one member of each pair received an injection of 2 mM  $\text{NaMoO}_4$ ; 0.15  $\mu\text{Ci}$   $2\text{-}^{14}\text{C}$ -acetate was then injected into each vial through the stopper and the vials were incubated for 1 h. Microbial activity was terminated by the addition of 0.5 mL 1 M HCl.

Samples were analyzed using a gas chromatograph (GC; GC-8A, Shimadzu, Inc., Columbia, MD) coupled with a gas proportional counter (GC-RAM, IN/US Systems, Inc., Brandon, FL).  $\text{CO}_2$  and  $\text{CH}_4$  were separated in the GC (column: Hayesep Q 80/100,  $8' \times 1/8''$  SS tubing; Grace Davison Discovery Sciences, Deerfield, IL), which was isothermal with a column temperature of 35 °C and an injection port temperature of 100 °C. After leaving the GC, samples passed through a pyrolytic column, kept at 750 °C, which combusted all  $\text{CH}_4$  to  $\text{CO}_2$ , prior to samples entering the gas proportional counter. Signal output from the gas proportional counter was plotted as counts per second versus time, and radioactive gases were quantified by peak area.  $\text{CH}_4$  peaks were indicative of methanogenesis, while  $\text{CO}_2$  peaks were indicative of non-methanogenic respiration. If  $\text{CO}_2$  production dropped sharply with the introduction of molybdate in a given sample, that sample was assumed to have sulfate reduction as its dominant terminal electron accepting process (TEAP). If  $\text{CO}_2$  production did not change significantly with the introduction of molybdate, a sample was assumed to have iron reduction as its dominant TEAP, as iron is the next most abundant electron acceptor in this system, after sulfate. Any samples with a preponderance of methane were assumed to be methanogenic.

## Statistical analysis

Stepwise and multiple linear regression was carried out using R (R Core Team 2013). Stepwise linear regression was carried out using the stepAIC() function in the MASS package. The variables used as potential explanatory variables for methylation rate potential in the stepwise linear regression are listed in Table S4, with the exception of depth below the sediment-water interface, which was also included as a variable.

## Results

### Total mercury, methylmercury, and DOC

Total mercury, methylmercury, and DOC concentrations were highly variable (Table 1; Fig. 2), which is consistent with the highly variable groundwater flow paths and source regions at the Allequash Creek site (Pint et al. 2003; Walker et al. 2003; Lowry et al. 2007; Kerr et al. 2008). In spite of the high variability, several trends were apparent in the data. Methylmercury and DOC concentrations were generally

higher during the summer field campaigns than those during the fall and winter campaigns, and were higher in the middle wetland than those in the upper springs (Fig. S1—MeHg; Fig. S2—DOC). When we aggregated the dataset over all seasonal sampling campaigns, we observed significant correlations between porewater MeHg and DOC at each site (upper springs:  $r^2 = 0.540$ ,  $p < 0.001$ ; middle wetland:  $r^2 = 0.490$ ,  $p < 0.001$ ; Fig. 3a), as well as a significant correlation when we pooled data from both sites ( $r^2 = 0.489$ ,  $p < 0.001$ ; Table S3).

Porewater HgT concentrations were seasonally variable (Fig. 2), but did not exhibit a clear seasonal trend across all sampling dates. Porewater MeHg did not correlate strongly with porewater HgT (Fig. 3b); however, porewater HgT was correlated with DOC ( $r^2 = 0.135$ ,  $p = 0.02$ ; Table S3). There was a weak positive correlation between methylation rate potentials and porewater HgT ( $r^2 = 0.094$ ,  $p = 0.054$ ).

Strong, Hg-binding organic ligands, a subset of DOC, did not contribute strongly to Hg speciation at either site. The measured concentrations of ligands (Table S2) were too low relative to sulfide concentrations to make a significant contribution to Hg speciation, in spite of the Hg-ligand complex

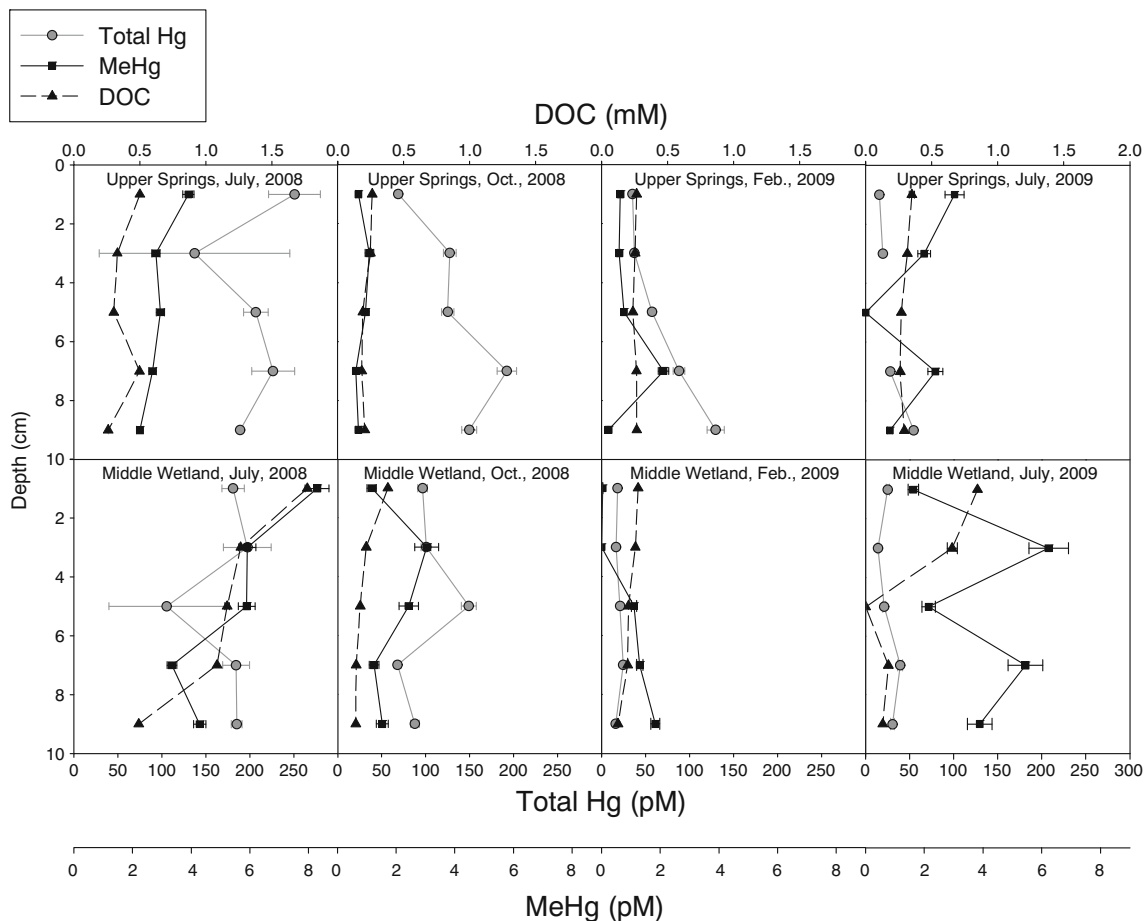


**Fig. 2** Porewater total mercury, methylmercury, and dissolved organic carbon (DOC) depth profiles from the four sampling campaigns

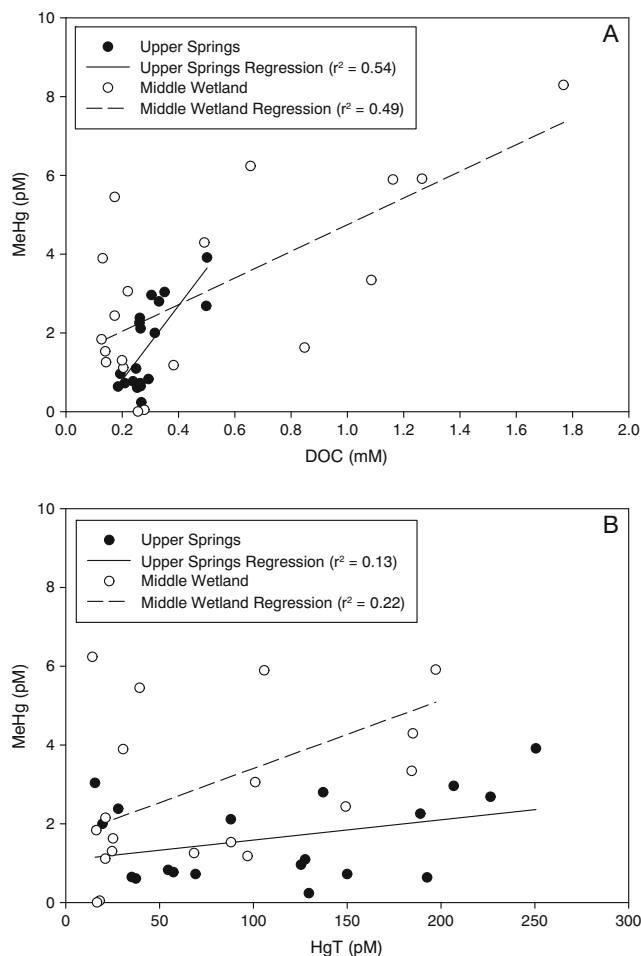


**Fig. 3** Linear regression analysis of MeHg versus DOC concentrations (a) and MeHg versus HgT (b)

having a higher stability constant. We confirmed the minor role of these ligands using equilibrium speciation modeling, demonstrating that the concentration of the Hg-ligand complex is many orders of magnitude lower than Hg-sulfide complexes (Fig. S7).

**Iron and sulfide**

We measured sulfide and total dissolved sulfur concentrations and reduced and total dissolved iron concentrations as indicators of sulfate- and iron-reducing conditions in the hyporheic sediments. More-reducing conditions are indicated by dissolved sulfide and Fe(II) representing a larger proportion of total dissolved sulfur and iron, respectively. Depth profiles of these two constituents (Figs. 4 and 5) indicate that the depth at which reducing conditions dominated was highly variable, both by site and by season; however, there was relatively good agreement between indicators about the depth of the redox boundary. In general, reducing conditions dominated the deeper portions of the sediment at the middle wetland site (below 2 cm for sulfide, below 4 cm for iron), while at the

upper springs site, to the extent that reducing conditions varied down-core, they occurred primarily in the middle of the depth profile, between 2 and 6 cm.

Concentrations of porewater sulfide and Fe(II) were the lowest during the October sampling campaign and had peaks that varied seasonally by site and constituent (Figs. S3 and S4). In addition to the seasonal variability in porewater sulfide and Fe(II), we observed inter-annual variability, with differences between the July, 2008 and July, 2009 concentration ranges of both constituents at both sites. The inter-annual variability may be partially explained by differences in flow. The U.S. Geological Survey stream gauge 05357206, located in Allequash Creek, several hundred meters downstream of the middle wetland site, measured a monthly mean discharge of  $0.086 \text{ m}^3 \text{ s}^{-1}$  in July, 2008 and  $0.041 \text{ m}^3 \text{ s}^{-1}$  in July, 2009. Although the gauge measures surface flow and the sulfide and Fe(II) measurements were made in porewater samples, the more than twofold difference in surface water flow implies a difference in groundwater flow and this groundwater-dominated site.

Given the sulfidic environment present at both sampling sites, mercury speciation and bioavailability is predicted to be controlled by sulfide concentration and the dominant Hg-sulfide species. Depending on the choice of stability constant chosen for the neutral  $\text{HgS}^0$  complex, the dominant Hg-sulfide species is either expected to be  $\text{HgHS}_2^-$  (not bioavailable) or  $\text{HgS}^0$  (bioavailable) (Fig. S8) (Benoit et al. 1999b, a).

**Methylation and demethylation rate potentials**

There was no significant difference between the upper springs and middle wetland sites in methylation rate potentials ( $t = -1.42$ ;  $p = 0.17$ ) or demethylation rate potentials ( $t = 1.73$ ;  $p = 0.095$ ). Methylation and demethylation rate potentials (Fig. 6) showed a seasonal trend, with the rates measured during the winter sampling campaign being consistently low relative to other seasons (Fig. S5). The highest methylation rate potential was observed at 7 cm in the middle wetland in July, 2008 (Fig. 6). This is in contrast to other studies showing a methylation peak closer to the sediment-water interface (Korthals and Winfrey 1987; Gilmour et al. 1992, 1998; Langer et al. 2001; Marvin-DiPasquale and Agee 2003). Demethylation rate potentials were higher than methylation rate potentials in almost every sample analyzed, and showed less seasonal variation (Fig. 6).

Methylation rate potentials were most strongly correlated with acid-volatile sulfide, DOC, porewater Fe(II), and porewater total dissolved Fe (Table 2). These variables, along with porewater HgT and porewater MeHg, were selected by stepwise linear regression as the most significant explanatory variables for methylation rate potentials, with a multiple  $r^2$  value of 0.5096 ( $p = 0.004$ ).

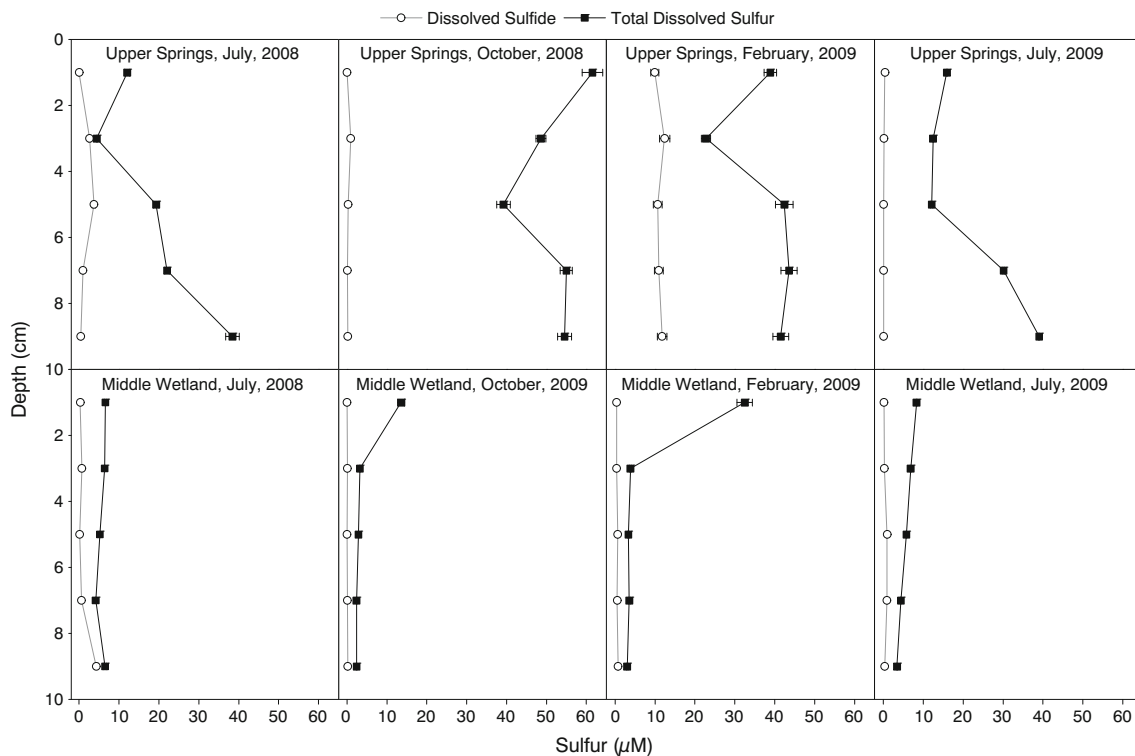


**Fig. 4** Dissolved sulfide and total dissolved sulfur depth profiles from the four sampling campaigns

Although no univariate correlation was observed between methylation rate potentials and either total dissolved iron or Fe(II), the highest methylation rate potentials occurred at depths where reducing conditions dominated (as indicated

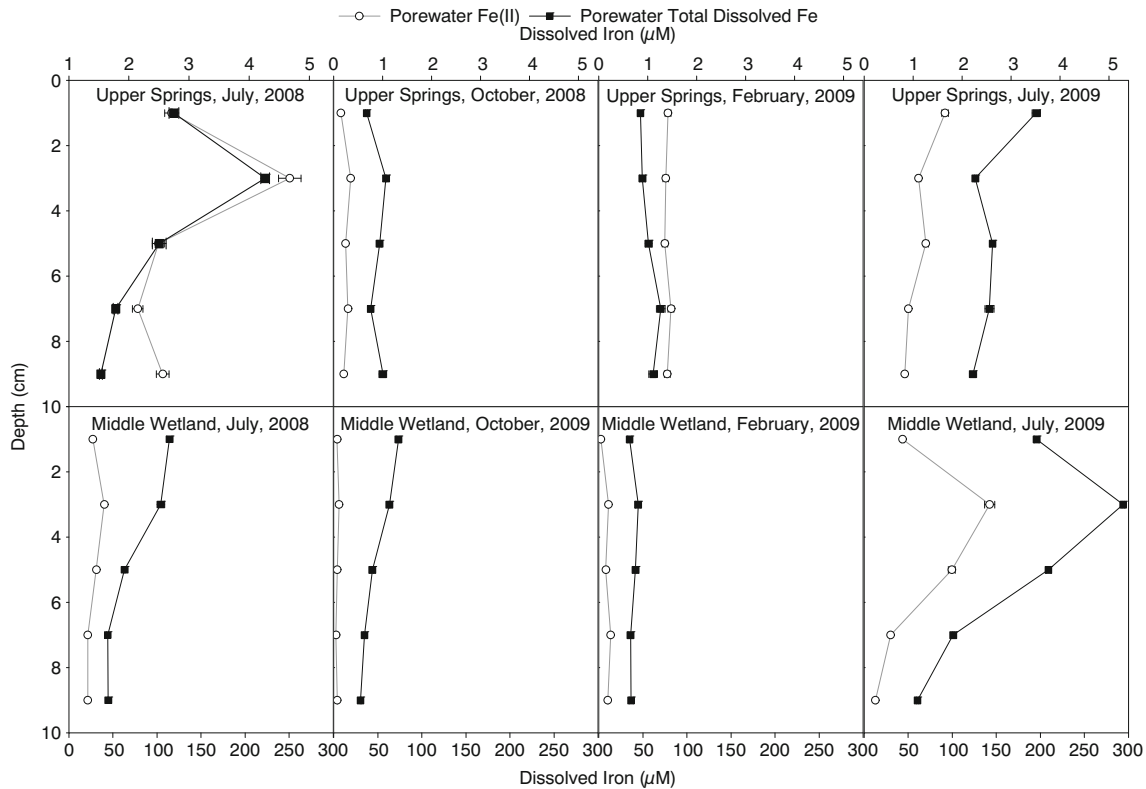


**Fig. 5** Porewater dissolved Fe(II) and total dissolved Fe depth profiles from the four sampling campaigns. Where the concentration of Fe(II) is greater than the concentration of total dissolved Fe, it should be assumed that Fe(II) accounts for 100% of dissolved Fe



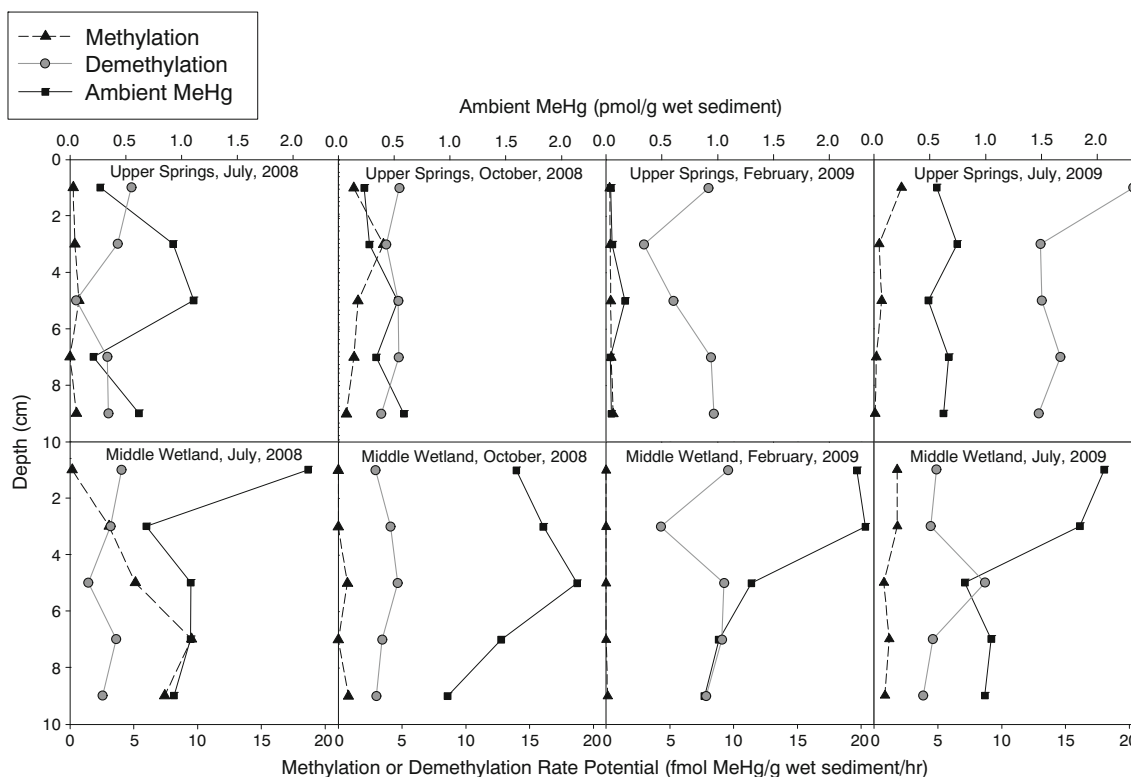


**Fig. 6** Depth profiles of methylation and demethylation rate potentials and ambient methylmercury concentrations, measured in whole sediment

by Fe depth profiles) or where conditions were more reducing than in the rest of the core (Figs. 4, 5, and 6). The lowest concentrations of porewater sulfide and Fe(II) were not observed during the February sampling campaign, when porewater temperatures and methylation rate potentials were the lowest (Figs. S3 and S4, respectively), but rather during the October campaign, indicating that porewater temperature also likely plays a role in controlling methylation rate potentials.

The relationship between methylation rate potentials and DOC is supported by univariate regression analysis of the pooled data from both sites, showing a significant positive correlation between DOC and methylation rate potentials

( $r = 0.433, p = 0.005$ ; Table S3). When broken down by site, however, this relationship is no longer significant: at the upper springs site (Fig. 7a), no correlation exists, and while there is a weak relationship between the two factors at the middle wetland site, it is primarily driven by a few high points (Fig. 7b). The significant correlation between porewater MeHg and DOC (Fig. 3a) also supports the conclusions of the multivariate regression, but may have been driven by the high points at the middle wetland site. The fact that the relationship between methylation rate potentials and DOC is only significant when considering pooled data is consistent with our understanding of this as a highly variable site, in which trends are only apparent with averaging to smooth out spatial heterogeneity.

**Table 2** Stepwise linear regression results. Multiple  $r^2 = 0.5096, p = 0.004$

	Coefficient	Standard error
(Intercept)	-0.0024763	0.0142409
AVS	0.2269535***	0.0582940
DOC	0.0746650**	0.0297901
Porewater Fe(II)	0.0015439**	0.0007285
Porewater HgT	0.0001956	0.0001248
Porewater MeHg	-0.0116629*	0.0061419
Porewater total dissolved Fe	-0.0007422**	0.0003286

\*\*\* $p < 0.001$ ; \*\* $p < 0.05$ ; \* $p < 0.1$

**Terminal electron accepting processes (TEAPS)**

Measurements of TEAPs indicated that the middle wetland site was primarily methanogenic, with typically small but varying production of CO<sub>2</sub> from sulfate- and iron-reducing bacteria (Fig. 8). There were several instances in the middle wetland samples when the addition of molybdate, a sulfate-reduction inhibitor, led to an increase in the production of labeled CO<sub>2</sub>. A rise in CO<sub>2</sub> production in the absence of sulfate reduction indicates that a different TEAP, most likely iron reduction, was the most prevalent non-methanogenic TEAP, and that this pathway was stimulated by the inhibition of sulfate reduction. There were also instances in these samples,

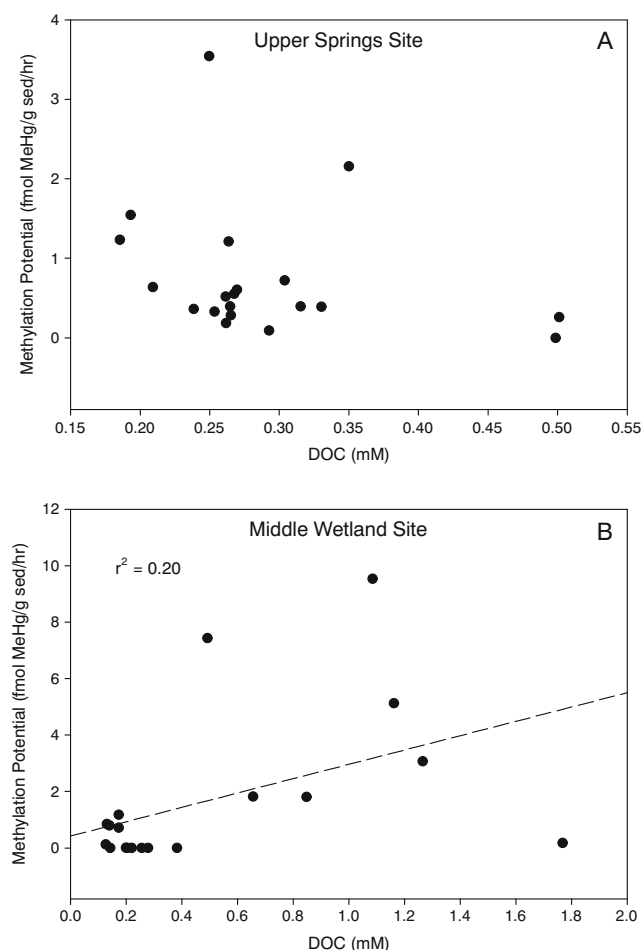


**Fig. 7** Plots of methylation rate potential versus dissolved organic carbon (DOC) at the upper springs site (a) and middle wetland site (b), across all sampling dates

however, in which the addition of molybdate decreased labeled  $\text{CO}_2$  production, indicating that sulfate reduction was more prevalent than iron reduction. The shifting of dominant TEAPs between depth horizons and sampling sites is consistent with our understanding of the dynamic nature of the hyporheic zone geochemistry at this site (e.g., Morrice et al. 2000).

In the upper springs samples, non-methanogenic TEAPs were more prevalent than methanogenesis at all sampling times except for July, 2009 (Fig. 8). In these samples, sulfate reduction and iron reduction seemed to be occurring concurrently in the cores at most sampling times, with neither process clearly dominant. In most instances, the addition of molybdate led to only a small change in the production of labeled  $\text{CO}_2$ . In February, 2009, however, at all depth horizons below 0–2 cm, sulfate reduction was the dominant TEAP, as indicated by the dramatic drop in labeled  $\text{CO}_2$  production with the addition of molybdate.

## Discussion

We observed wide spatial and temporal variability in methylation rate potentials and MeHg concentrations (Fig. 6). The primary geochemical factors correlated with this variability were acid-volatile sulfide, DOC, porewater Fe(II), and porewater total dissolved Fe (Table 2). These factors are related primarily to microbial metabolism: the forms of iron and sulfide are either electron acceptors or reduced metabolic byproducts, and DOC can serve as a carbon source. There is a weaker correlation between methylation rate potentials and porewater HgT, indicating that this factor is not likely to be limiting the methylation process. There is also a weak correlation between methylation rate potentials and porewater MeHg, indicating that methylmercury production in this system is highly dynamic, spatially and temporally, leading to a spatial and/or temporal disconnect between the occurrence of MeHg production and the observation of porewater MeHg.

The observed patterns in methylation rate potentials, redox indicators, and DOC are likely due to the influence of geology on site geochemistry as well as season and porewater temperature. Geology is likely the primary driver of spatial heterogeneity at the Allequash Creek wetland site. In addition, demethylation rates may also play a key role in regulating methylmercury production at this site.

### Influence of geology on site geochemistry

We found that reducing conditions (indicated by the presence of detectable dissolved iron and sulfide) occurred at a wider range of depths at the upper springs site than at the middle wetland site, where they were more uniformly found in the deeper portions of the cores. The more spatially variable occurrence of reducing conditions at the upper springs site is consistent with the highly porous substrate at that site, allowing for more rapid changes in hyporheic conditions than that at the middle wetland site. Groundwater source region and flow path exert a strong influence on the chemistry of groundwater discharge in the Allequash Creek wetland, and that discharge (and recharge) is highly spatially variable within the creek (Pint et al. 2003; Walker et al. 2003; Lowry et al. 2007; Kerr et al. 2008). Groundwater discharging to the upper springs site is predicted to have spent less time in the subsurface (>25–50 years) than groundwater discharging to the middle wetland site (50–150 years), and is predicted to be less reducing than older groundwater (Pint et al. 2003). The more-porous substrate at the upper springs site allows for more subsurface mixing of surface water and groundwater. We expect that this combination of less-reducing groundwater and more-porous substrate was the cause of the high variability in the occurrence of reducing conditions at the upper springs site.

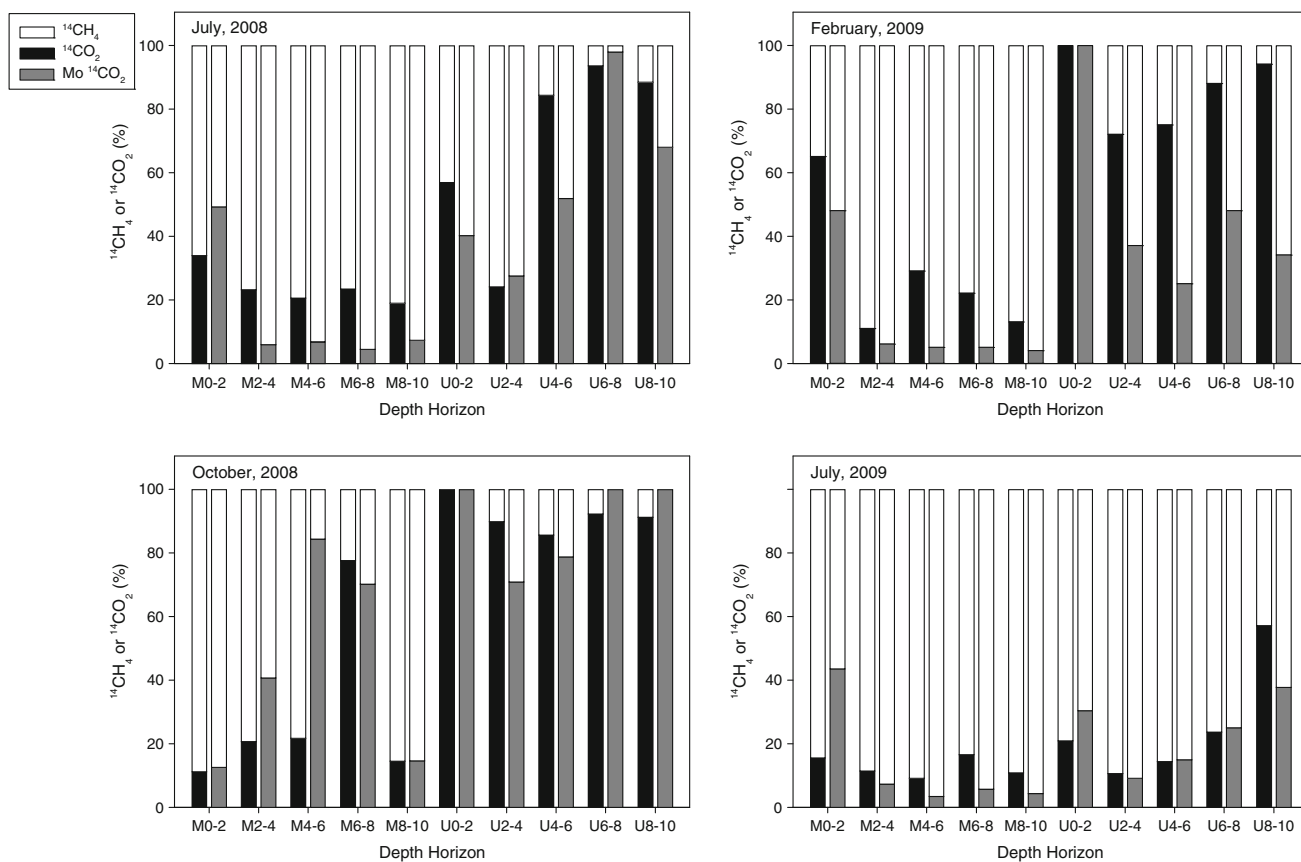


**Fig. 8** Terminal electron accepting process measurements from the four sampling campaigns. *M* middle wetland site, *U* upper springs site. Numbers in depth horizon labels denote depth (in cm) below the sediment-water interface

The high degree of hyporheic mixing, especially at the upper springs site, is expected to support a diversity of microbial functional groups and continuously refresh the supply of electron acceptors to support their respiration. In other studies, methylmercury production was the highest in the surface sediments where hyporheic mixing was the highest (Langer et al. 2001; Bouchet et al. 2011); however, at this site, we observed few peaks in methylation rates in surface sediments. One explanation for this difference is that the dominant TEAP in the surface sediments at this site varies both seasonally and with depth between sulfate and iron reduction and methanogenesis. While the first two processes are known to methylate mercury at comparatively high rates (Compeau and Bartha 1985; Warner et al. 2003; Fleming et al. 2006; Kerin et al. 2006), lower methylation rates or inhibition of methylation is associated with methanogenesis (Compeau and Bartha 1985; Gilmour et al. 2013). The persistent presence and, in some seasons, dominance of methanogenic bacterial metabolism may be limiting the production of methylmercury in surface sediments with high hyporheic mixing. Another possible explanation for the lack of high mercury methylation rates in the upper springs sediments is that the large amount of mixing at this site results in dissolved oxygen levels in the surface sediments that prevent anaerobic, Hg-methylating bacteria from

reaching high rates of metabolism. However, dissolved oxygen, which was not measured in this study, would also limit methanogenesis, something the TEAP measurements suggest is occurring.

There were no clear correlations between dominant TEAPs (Fig. 8) and net methylation rate potentials (Fig. 6) on any of the sampling dates. This lack of correlation is most likely due to the dominance of methanogenesis in the majority of the samples measured. It is likely that sulfate and/or iron reduction are occurring simultaneously with methanogenesis at many depths, as has been observed previously in freshwater wetland sediments (Roden and Wetzel 1996), and that the competition between the pathways limits the dominance of any one of them. Although the dominant TEAP no doubt exerts strong control over methylmercury production rates (Hamelin et al. 2011), the lack of a clearly dominant process and the prevalence of methanogenesis in many samples makes it difficult to directly associate the TEAP measurements with increases or decreases in the net methylation rate.

There were significant correlations between mercury methylation rates and AVS in both the univariate ( $r^2 = 0.258$ ,  $p = 0.001$ ; Table S3) and multivariate (coefficient = 0.227;  $p < 0.001$ ; Table 2) regressions, but no significant correlation between methylation rates and porewater sulfide

concentrations ( $r^2 = 0.004$ ,  $p = 0.71$ ; Table S3). AVS consists primarily of iron sulfide (FeS) (Liu et al. 2008), which is known to immobilize dissolved Hg(II) and remove it from the water column, a process that should lower the bioavailable Hg concentration and decrease methylation rates (Morse and Arakaki 1993; Mehrotra et al. 2003; Mehrotra and Sedlak 2005; Jeong et al. 2010). In this system, however, porewater inorganic Hg concentration is probably not the primary factor limiting methylmercury production. The positive correlation between methylation rate potentials and AVS, but not porewater sulfide, is probably due to the fact that sulfide produced by the mercury-methylating, sulfate-reducing bacteria is being scavenged by iron and precipitating as AVS. We did not observe a correlation between methylation rate potentials and total dissolved sulfur or the percentage of total dissolved sulfur represented by sulfide (Table S3).

As discussed above, the choice of stability constant for the neutral  $\text{HgS}^0$  complex determines whether a bioavailable ( $\text{HgS}^0$ ) or unavailable ( $\text{HgHS}_2^-$ ) Hg species is predicted to dominate Hg-sulfide speciation. However, the theoretical  $\text{HgS}^0_{(\text{aq})}$  complex has been shown to actually include both colloidal and dissolved species, the solubility of which is controlled by dissolved organic matter (Miller et al. 2007; Deonaraine and Hsu-Kim 2009; Slowey 2010; Graham et al. 2012). Sulfate-reducing bacteria are capable of methylating both dissolved HgS and HgS nanoparticles (Zhang et al. 2012); thus, regardless of which stability constant is used and whether dissolved neutral HgS species are present, the presence in either case of nanoparticulate  $\text{HgS}_{(\text{s})}$  allows methylation to occur. Additionally, it is possible that microbial uptake of inorganic Hg(II) occurs via kinetically limited intermediate (non-equilibrium) species, as has been suggested by Slowey (2010). This would allow for mercury methylation to occur in systems in which no bioavailable Hg-S species are predicted.

The weak but significant relationship between methylation rates and porewater Fe(II) in the multivariate regression (coefficient = 0.002,  $p < 0.05$ ; Table 2) suggests that iron reduction, in addition to sulfate reduction, may be playing a role in mercury methylation. The variability in the iron and sulfur depth profiles as well as in the zones of dominance of sulfate and iron reduction, indicates that Hg(II) speciation is constantly in flux. It is likely that this constant shifting in speciation was a major contributor to the high variation in methylmercury production.

### Season (temperature)

MeHg and DOC concentrations showed a seasonal trend and were significantly correlated. Concentrations of both constituents were generally higher during the summer than those during the fall and winter, suggesting that the sources of these constituents are less active in colder months when water

temperatures are lower. The source of DOC is most likely decaying organic matter and the source of MeHg is most likely microbial methylation of inorganic mercury. The correlation between MeHg and DOC is consistent with observations from a number of other sites (Driscoll et al. 1995, 1998; Babiarz et al. 1998; Shanley et al. 2008; Tsui and Finlay 2011) and suggests either a common source or a role for DOC in the production of MeHg in this system.

The seasonal trend observed in methylation rate potentials is also partially explained by the influence of porewater temperatures on microbial metabolic rates. However, the methylation rate minimum did not coincide with the minimum observed concentrations of indicators of microbial metabolism, porewater sulfide and Fe(II) (Figs. S3 and S4, respectively), suggesting a decoupling of mercury methylation and the buildup of reduced electron acceptors. The low methylation rate potentials in February coincide with our observation of the lowest porewater MeHg concentrations, suggesting that the MeHg measured in porewater is primarily produced in situ, rather than desorbed from the solid phase or transported from a source region elsewhere.

A possible explanation for low mercury methylation rate potentials in the winter is that decreased microbial activity results from lowered hyporheic mixing, rather than from low temperatures. A decline in mixing would result in a less-frequently refreshed supply of oxidized electron acceptors available to methylating iron- and sulfate-reducing bacteria, and would allow for more buildup of reduced species. This mechanism could explain why the concentrations of porewater iron and sulfide were not at their lowest in February.

### Demethylation

Demethylation rate potentials were higher and less seasonally variable than methylation rate potentials. This finding is consistent with studies showing that demethylation is carried out by a larger consortium of microbial species than methylation (Benoit et al. 2003; Heyes et al. 2006; Merritt and Amirbahman 2009) and that demethylation rates are generally higher than methylation rates (Pak and Bartha 1998; Bridou et al. 2011). High demethylation rate potentials may mean that the low concentrations of methylmercury generally found in the sediments of the Allequash Creek wetland are due largely to high demethylation rates limiting the net production of methylmercury. However, there are several caveats to consider when assessing the influence of demethylation rate potentials relative to methylation rate potentials. Demethylation rate potentials may overestimate true, in situ transformation rates to a greater degree than methylation rate potentials. Because both measurements involve the addition of an exogenous Hg spike, they are assumed to overestimate in situ processes, but the degree to which this occurs is unknown. Although relative differences in rate potentials can be assumed to correlate to

differences in the in situ processes, a demethylation rate potential that is higher than a methylation rate potential may not denote an in situ demethylation rate higher than the methylation rate. However, the fact that the demethylation rate potential measurements were consistently high and did not vary substantially by season suggests that demethylation plays an important role in regulating net methylmercury production and export.

## Conclusions

Methylmercury production in this system was highly variable and was controlled primarily by acid-volatile sulfide, DOC, porewater Fe(II), and porewater total dissolved Fe. All of these controlling factors are involved in microbial metabolism and influence the speciation and bioavailability of mercury. Although there was high spatial variability in methylmercury production, as indicated by the depth profiles of methylation rate potentials, there were no significant differences between the upper springs and middle wetland sites. Total mercury concentrations had no significant influence on mercury methylation rate potentials.

Methylmercury production followed a clear seasonal trend, with the lowest rates generally occurring in the winter, when porewater temperatures were the lowest. The high, relatively consistent demethylation rates highlight the important role that in situ demethylation plays in regulating net methylmercury production and export. As with the observed variation in geochemistry, the variability in TEAPs and the prevalence of methanogenesis explains some fluctuation in methylation rates. The TEAP data paint a picture of a system continuously in flux, in which no microbial consortium is able to establish metabolic dominance for a significant period of time, contributing to the fluctuations in methylation rates. The findings of this study demonstrate the key role of iron, sulfide, and DOC in controlling mercury methylation in the Allequash Creek wetland and add to our understanding of the complexity and variability of hyporheic zone biogeochemistry in groundwater-dominated peat wetlands.

**Acknowledgements** We thank Brice Gu, Krysta Koralesky, Amy Kolpin, and Emily Kara for the field and lab assistance, and the University of Wisconsin – Madison Trout Lake Station for the lab space, vehicle use, and logistical support. This work was funded in part by the Wisconsin Groundwater Research and Monitoring Program (Grants WR09R003 and WR07R008). Joel Creswell was supported in part by an EPA STAR Fellowship (FP-91687801). EPA has not endorsed this publication and the views expressed herein may not reflect the views of the EPA.

## References

- Babiarz CL, Hurley JP, Benoit JM et al (1998) Seasonal influences on partitioning and transport of total and methylmercury in rivers from contrasting watersheds. *Biogeochemistry* 41:237–257. doi:10.1023/A:1005940630948
- Barkay T, Gillman M, Turner RR (1997) Effects of dissolved organic carbon and salinity on bioavailability of mercury. *Appl Environ Microbiol* 63:4267–4271
- Benoit JM, Gilmour CC, Heyes A et al (2003) Geochemical and biological controls over methylmercury production and degradation in aquatic ecosystems. In: Cai Y, Braids OC (eds) *Biogeochemistry of environmentally important trace elements*. Amer Chemical Soc, Washington, pp 262–297
- Benoit JM, Gilmour CC, Mason RP (2001) Aspects of bioavailability of mercury for methylation in pure cultures of *Desulfobulbus propionicus* (1pr3). *Appl Environ Microbiol* 67:51–58. doi:10.1128/AEM.67.1.51-58.2001
- Benoit JM, Gilmour CC, Mason RP, Heyes A (1999a) Sulfide controls on mercury speciation and bioavailability to methylating bacteria in sediment pore waters. *Environ Sci Technol* 33:951–957. doi:10.1021/es9808200
- Benoit JM, Mason RP, Gilmour CC (1999b) Estimation of mercury-sulfide speciation in sediment pore waters using octanol–water partitioning and implications for availability to methylating bacteria. *Environ Toxicol Chem* 18:2138–2141. doi:10.1897/1551-5028(1999)018<2138:EOMSSI>2.3.CO;2
- Bloom N (1992) On the chemical form of mercury in edible fish and marine invertebrate tissue. *Can J Fish Aquat Sci* 49:1010–1017. doi:10.1139/f92-113
- Blum JD, Bergquist BA (2007) Reporting of variations in the natural isotopic composition of mercury. *Anal Bioanal Chem* 388:353–359. doi:10.1007/s00216-007-1236-9
- Bouchet S, Bridou R, Tessier E et al (2011) An experimental approach to investigate mercury species transformations under redox oscillations in coastal sediments. *Mar Environ Res* 71:1–9. doi:10.1016/j.marenvres.2010.09.001
- Bridou R, Monperrus M, Gonzalez PR et al (2011) Simultaneous determination of mercury methylation and demethylation capacities of various sulfate-reducing bacteria using species-specific isotopic tracers. *Environ Toxicol Chem* 30:337–344. doi:10.1002/etc.395
- Cline JD (1969) Spectrophotometric determination of hydrogen sulfide in natural waters. *Limnol Oceanogr* 14:454–458
- Compeau GC, Bartha R (1985) Sulfate-reducing bacteria: principal methylators of mercury in anoxic estuarine sediment. *Appl Environ Microbiol* 50:498–502
- Creswell JE, Kerr SC, Meyer MH et al (2008) Factors controlling temporal and spatial distribution of total mercury and methylmercury in hyporheic sediments of the Allequash Creek wetland, northern Wisconsin. *J Geophys Res Biogeosciences*. doi:10.1029/2008JG000742
- Deonaraine A, Hsu-Kim H (2009) Precipitation of mercuric sulfide nanoparticles in NOM-containing water: implications for the natural environment. *Environ Sci Technol* 43:2368–2373. doi:10.1021/es803130h
- Driscoll C, Blette V, Yan C et al (1995) The role of dissolved organic carbon in the chemistry and bioavailability of mercury in remote Adirondack Lakes. *Water Air Soil Pollut* 80:499–508. doi:10.1007/BF01189700
- Driscoll CT, Holsapple J, Schofield CL, Munson R (1998) The chemistry and transport of mercury in a small wetland in the Adirondack region of New York, USA. *Biogeochemistry* 40:137–146. doi:10.1023/A:1005989229089
- Drott A, Lambertsson L, Björn E, Skyllberg U (2007) Importance of dissolved neutral mercury sulfides for methyl mercury production

- in contaminated sediments. *Environ Sci Technol* 41:2270–2276. doi:10.1021/es061724z
- Fleming EJ, Mack EE, Green PG, Nelson DC (2006) Mercury methylation from unexpected sources: molybdate-inhibited freshwater sediments and an iron-reducing bacterium. *Appl Environ Microbiol* 72:457–464. doi:10.1128/AEM.72.1.457-464.2006
- Fossing H, Jørgensen BB (1989) Measurement of bacterial sulfate reduction in sediments: evaluation of a single-step chromium reduction method. *Biogeochemistry* 8:205–222
- Gerringa LJA, Herman PMJ, Poortvliet TCW (1995) Comparison of the linear van den Berg/Ružić transformation and a non-linear fit of the Langmuir isotherm applied to Cu speciation data in the estuarine environment. *Mar Chem* 48:131–142. doi:10.1016/0304-4203(94)00041-B
- Gilmour C, Riedel GS, Ederington MC et al (1998) Methylmercury concentrations and production rates across a trophic gradient in the northern Everglades. *Biogeochemistry* 40:327–345. doi:10.1023/A:1005972708616
- Gilmour CC, Henry EA, Mitchell R (1992) Sulfate stimulation of mercury methylation in freshwater sediments. *Environ Sci Technol* 26:2281–2287. doi:10.1021/es00035a029
- Gilmour CC, Podar M, Bullock AL et al (2013) Mercury methylation by novel microorganisms from new environments. *Environ Sci Technol* 47:11810–11820. doi:10.1021/es403075t
- Graham AM, Aiken GR, Gilmour CC (2012) Dissolved organic matter enhances microbial mercury methylation under sulfidic conditions. *Env Sci Technol* 46:2715–2723. doi:10.1021/es203658f
- Hamelin S, Amyot M, Barkay T et al (2011) Methanogens: principal methylators of mercury in Lake Periphyton. *Environ Sci Technol* 45:7693–7700. doi:10.1021/es2010072
- Hammerschmidt CR, Fitzgerald WF (2004) Geochemical controls on the production and distribution of methylmercury in near-shore marine sediments. *Environ Sci Technol* 38:1487–1495. doi:10.1021/es034528q
- Heyes A, Mason RP, Kim E-H, Sunderland E (2006) Mercury methylation in estuaries: insights from using measuring rates using stable mercury isotopes. *Mar Chem* 102:134–147. doi:10.1016/j.marchem.2005.09.018
- Hintelmann H, Evans RD (1997) Application of stable isotopes in environmental tracer studies—measurement of monomethylmercury (CH<sub>3</sub>Hg<sup>+</sup>) by isotope dilution ICP-MS and detection of species transformation. *Fresenius J Anal Chem* 358:378–385. doi:10.1007/s002160050433
- Hintelmann H, Evans RD, Villeneuve JY (1995) Measurement of mercury methylation in sediments by using enriched stable mercury isotopes combined with methylmercury determination by gas chromatography-inductively coupled plasma mass spectrometry. *J Anal At Spectrom* 10:619. doi:10.1039/ja9951000619
- Hoffmann SR (2002) Strong binding of copper, zinc, and lead to colloids and natural organic matter in rivers. Ph.D., University of Wisconsin - Madison
- Horvat M, Bloom NS, Liang L (1993) Comparison of distillation with other current isolation methods for the determination of methyl mercury compounds in low level environmental samples: part 1. Sediments. *Anal Chim Acta* 281:135–152. doi:10.1016/0003-2670(93)85348-N
- Hurley JP, Benoit JM, Babiarz CL et al (1995) Influences of watershed characteristics on mercury levels in Wisconsin rivers. *Environ Sci Technol* 29:1867–1875. doi:10.1021/es00007a026
- Jeong HY, Sun K, Hayes KF (2010) Microscopic and spectroscopic characterization of Hg(II) immobilization by mackinawite (FeS). *Environ Sci Technol* 44:7476–7483. doi:10.1021/es100808y
- Kerin EJ, Gilmour CC, Roden E et al (2006) Mercury methylation by dissimilatory iron-reducing bacteria. *Appl Environ Microbiol* 72:7919–7921. doi:10.1128/AEM.01602-06
- Kerr SC, Shafer MM, Overdier J, Armstrong DE (2008) Hydrologic and biogeochemical controls on trace element export from northern Wisconsin wetlands. *Biogeochemistry* 89:273–294. doi:10.1007/s10533-008-9219-2
- Korthals ET, Winfrey MR (1987) Seasonal and spatial variations in mercury methylation and demethylation in an oligotrophic lake. *Appl Environ Microbiol* 53:2397–2404
- Krabbenhoft D, Benoit J, Babiarz C et al (1995) Mercury cycling in the Allequash Creek watershed, northern Wisconsin. *Water Air Soil Pollut* 80:425–433. doi:10.1007/BF01189692
- Lamborg CH, Tseng CM, Fitzgerald WF et al (2003) Determination of the mercury complexation characteristics of dissolved organic matter in natural waters with “reducible Hg” titrations. *Environ Sci Technol* 37:3316–3322. doi:10.1021/es0264394
- Langer CS, Fitzgerald WF, Visscher PT, Vandal GM (2001) Biogeochemical cycling of methylmercury at Barn Island salt marsh, Stonington, CT, USA. *Wetl Ecol Manag* 9:295–310. doi:10.1023/A:1011816819369
- Liu J, Valsaraj KT, Devai I, DeLaune RD (2008) Immobilization of aqueous Hg(II) by mackinawite (FeS). *J Hazard Mater* 157:432–440. doi:10.1016/j.jhazmat.2008.01.006
- Lovley DR (1997) Potential for anaerobic bioremediation of BTEX in petroleum-contaminated aquifers. *J Ind Microbiol Biotechnol* 18:75–81. doi:10.1038/sj.jim.2900246
- Lovley DR, Phillips EJ (1986) Availability of ferric iron for microbial reduction in bottom sediments of the freshwater tidal Potomac River. *Appl Environ Microbiol* 52:751–757
- Lowry CS, Walker JF, Hunt RJ, Anderson MP (2007) Identifying spatial variability of groundwater discharge in a wetland stream using a distributed temperature sensor. *Water Resour Res* 43:n/a-n/a. doi:10.1029/2007WR006145
- Marvin-DiPasquale M, Agee JL (2003) Microbial mercury cycling in sediments of the San Francisco Bay-Delta. *Estuaries* 26:1517–1528. doi:10.1007/BF02803660
- Mehrotra AS, Home AJ, Sedlak DL (2003) Reduction of net mercury methylation by iron in *Desulfobulbus propionicus* (1pr3) cultures: implications for engineered wetlands. *Environ Sci Technol* 37:3018–3023. doi:10.1021/es0262838
- Mehrotra AS, Sedlak DL (2005) Decrease in net mercury methylation rates following iron amendment to anoxic wetland sediment slurries. *Environ Sci Technol* 39:2564–2570. doi:10.1021/es049096d
- Merritt KA, Amirbahman A (2009) Mercury methylation dynamics in estuarine and coastal marine environments—a critical review. *Earth-Sci Rev* 96:54–66. doi:10.1016/j.earscirev.2009.06.002
- Miller CL, Mason RP, Gilmour CC, Heyes A (2007) Influence of dissolved organic matter on the complexation of mercury under sulfidic conditions. *Environ Toxicol Chem* 26:624–633. doi:10.1897/06-375R.1
- Miskimmin B, Rudd J, Kelly C (1992) Influence of dissolved organic carbon, pH, and microbial respiration rates on mercury methylation and demethylation in lake water. *Can J Fish Aquat Sci* 49:17–22. doi:10.1139/f92-002
- Mitchell CPJ, Branfireun BA, Kolka RK (2008b) Spatial characteristics of net methylmercury production hot spots in peatlands. *Environ Sci Technol* 42:1010–1016. doi:10.1021/es0704986
- Mitchell CPJ, Branfireun BA, Kolka RK (2008a) Assessing sulfate and carbon controls on net methylmercury production in peatlands: an in situ mesocosm approach. *Appl Geochem* 23:503–518. doi:10.1016/j.apgeochem.2007.12.020
- Morrice JA, Dahm CN, Valett HM et al (2000) Terminal electron accepting processes in the alluvial sediments of a headwater stream. *J North Am Benthol Soc* 19:593–608. doi:10.2307/1468119
- Morse JW, Arakaki T (1993) Adsorption and coprecipitation of divalent metals with mackinawite (FeS). *Geochim Cosmochim Acta* 57:3635–3640. doi:10.1016/0016-7037(93)90145-M

- Olson ML, Cleckner LB, Hurley JP et al (1997) Resolution of matrix effects on analysis of total and methyl mercury in aqueous samples from the Florida Everglades. *Fresenius J Anal Chem* 358:392–396. doi:10.1007/s002160050435
- Pak K-R, Bartha R (1998) Mercury methylation and demethylation in anoxic lake sediments and by strictly anaerobic bacteria. *Appl Environ Microbiol* 64:1013–1017
- Pint CD, Hunt RJ, Anderson MP (2003) Flowpath delineation and ground water age, Allequash Basin, Wisconsin. *Ground Water* 41:895–902. doi:10.1111/j.1745-6584.2003.tb02432.x
- Core Team R (2013) R: a language and environment for statistical computing. R Foundation for Statistical Computing, Vienna, Austria
- Ravichandran M (2004) Interactions between mercury and dissolved organic matter—a review. *Chemosphere* 55:319–331. doi:10.1016/j.chemosphere.2003.11.011
- Roden EE, Wetzel RG (1996) Organic carbon oxidation and suppression of methane production by microbial Fe(III) oxide reduction in vegetated and unvegetated freshwater wetland sediments. *Limnol Oceanogr* 41:1733–1748. doi:10.2307/2838658
- Schaefer JK, Morel FMM (2009) High methylation rates of mercury bound to cysteine by *Geobacter sulfurreducens*. *Nat Geosci* 2:123–126. doi:10.1038/ngeo412
- Schecher WD, McAvoy DC (2002) MINEQL+—a software environment for chemical equilibrium modeling. Environmental Research Software, Hallowell, Maine
- Shafer MM, Overdier JT, Phillips H et al (1999) Trace metal levels and partitioning in Wisconsin rivers. *Water Air Soil Pollut* 110:273–311. doi:10.1023/A:1005019521097
- Shanley JB, Alisa Mast M, Campbell DH et al (2008) Comparison of total mercury and methylmercury cycling at five sites using the small watershed approach. *Environ Pollut* 154:143–154. doi:10.1016/j.envpol.2007.12.031
- Skylberg U (2008) Competition among thiols and inorganic sulfides and polysulfides for Hg and MeHg in wetland soils and sediments under suboxic conditions: illumination of controversies and implications for MeHg net production. *J Geophys Res Biogeosciences*. doi:10.1029/2008JG000745
- Slowey AJ (2010) Rate of formation and dissolution of mercury sulfide nanoparticles: the dual role of natural organic matter. *Geochim Cosmochim Acta* 74:4693–4708. doi:10.1016/j.gca.2010.05.012
- St. Louis VL, Rudd JW, Kelly CA et al (1996) Production and loss of methylmercury and loss of total mercury from boreal forest catchments containing different types of wetlands. *Environ Sci Technol* 30:2719–2729. doi:10.1021/es950856h
- Stookey LL (1970) Ferrozine—a new spectrophotometric reagent for iron. *Anal Chem* 42:779–781. doi:10.1021/ac60289a016
- Tsui MTK, Finlay JC (2011) Influence of dissolved organic carbon on methylmercury bioavailability across Minnesota stream ecosystems. *Environ Sci Technol*. doi:10.1021/es200332f
- U.S. Environmental Protection Agency (2001a) Method 1630: methyl mercury in water by distillation, aqueous ethylation, purge and trap, and CVAFS. U.S. Environmental Protection Agency, Washington, D.C.
- U.S. Environmental Protection Agency (2002) Method 1631, revision E: mercury in water by oxidation, purge and trap, and cold vapor atomic fluorescence spectrometry
- U.S. Environmental Protection Agency (2001b) Appendix to Method 1631 total mercury in tissue, sludge, sediment, and soil by acid digestion and BrCl oxidation
- Viollier E, Inglett PW, Hunter K et al (2000) The ferrozine method revisited: Fe(II)/Fe(III) determination in natural waters. *Appl Geochem* 15:785–790. doi:10.1016/S0883-2927(99)00097-9
- Walker JF, Hunt RJ, Bullen TD et al (2003) Variability of isotope and major ion chemistry in the Allequash Basin, Wisconsin. *Ground Water* 41:883–894. doi:10.1111/j.1745-6584.2003.tb02431.x
- Warner KA, Roden EE, Bonzongo J-C (2003) Microbial mercury transformation in anoxic freshwater sediments under iron-reducing and other electron-accepting conditions. *Environ Sci Technol* 37:2159–2165. doi:10.1021/es0262939
- Zhang T, Kim B, Levard C et al (2012) Methylation of mercury by bacteria exposed to dissolved, nanoparticulate, and microparticulate mercuric sulfides. *Environ Sci Technol* 46:6950–6958. doi:10.1021/es203181m